Protein Engineering, Design & Selection vol. 20 no. 6 pp. 273–284, 2007
Published online June 26, 2007 doi:10.1093/protein/gzm020

Fusion of a recombinant antibody fragment with a homo-amino-acid polymer: effects on biophysical properties and prolonged plasma half-life

Martin Schlapschy[1], Ina Theobald[1], Hildegard Mack[1], Margret Schottelius[2], Hans-Jürgen Wester[2] and Arne Skerra[1,3]

[1]Lehrstuhl für Biologische Chemie, Technische Universität München, 85350 Freising-Weihenstephan, Germany and [2]Nuklearmedizinische Klinik und Poliklinik, Klinikum rechts der Isar, Technische Universität München, 81675 München, Germany

[3]To whom correspondence should be addressed.
E-mail: skerra@wzw.tum.de

Chemical conjugation of small recombinant proteins with polyethylene glycol (PEG) is an established strategy to extend their typically short circulation times to a therapeutically useful range. We have investigated the production of a genetic fusion with a glycine-rich homo-amino-acid polymer (HAP) as an alternative way to attach a solvated random chain with large hydrodynamic volume. The anti-HER2 Fab fragment 4D5 was used as a model system and fused with either 100 or 200 residue polymers of the repetitive sequence $(Gly_4Ser)_n$ to its light chain. Both fusion proteins were successfully produced in the periplasm of *Escherichia coli* and obtained as homogeneous preparations after two-step affinity chromatography via the His_6 tag fused to the heavy chain and the *Strep*-tag II fused to the extended light chain. Both modified Fab fragments showed binding activity towards the HER2 antigen indistinguishable from the conventional recombinant Fab fragment. When compared with the unfused Fab fragment, a significantly increased hydrodynamic volume, by ca. 120%, was observed during gel filtration for the 200 residue HAP fusion protein and, to a lesser extent, in the case of the 100 residue HAP. Difference CD measurements revealed a characteristic random coil spectrum for the 100 and 200 residue HAP fusion moieties. Finally, pharmacokinetic experiments were carried out in mice after radioiodination of the recombinant Fab fragments. Although the 100 residue HAP fusion showed a behavior very similar to the unfused Fab fragment, with a terminal plasma half-life of ca. 2 h, the 200 residue HAPylated Fab fragment gave rise to a significantly prolonged half-life of ca. 6 h. While this moderate effect may so far be most beneficial for specialized medical applications, such as *in vivo* imaging, the genetic engineering of optimized HAP sequences should yield pharmacokinetic properties similar to PEGylation, yet without necessitating *in vitro* modification steps.

Keywords: biopharmaceutical/hydrodynamic volume/kidney filtration/random coil/therapeutic protein

Introduction

Common plasma proteins such as human serum albumin (HSA) and immunoglobulins (Igs), including humanized antibodies, show long half-lives, typically of 2–3 weeks, which is attributable to their specific interaction with the neonatal Fc receptor (FcRn) and endosomal recycling (Ghetie and Ward, 2002). In contrast, most other proteins of pharmaceutical interest, in particular recombinant antibody fragments, hormones, interferons, etc., suffer from rapid clearance. This is particularly true for proteins whose size is below the threshold value for kidney filtration of about 70 kDa (Caliceti and Veronese, 2003). In these cases, the plasma half-life of an unmodified pharmaceutical protein may be considerably less than an hour, thus rendering it essentially useless for most therapeutic applications. In order to achieve sustained pharmacological action and also improved patient compliance, with required dosing intervals extending to several days or even weeks, two major strategies have been established for the purposes of biopharmaceutical drug development.

First, the recycling mechanism of natural plasma proteins has been employed by producing fusion proteins with the Fc portion of Igs, for example Enbrel®, a hybrid between the extracellular domain of TNFα receptor and human IgG1 (Goldenberg, 1999), or with serum albumin, for example Albuferon®, a corresponding fusion of IFN-α with HSA (Osborn *et al.*, 2002). Albumin with its high plasma concentration of 600 μM has also been utilized in an indirect manner, serving as carrier vehicle for biopharmaceuticals that are equipped with an albumin-binding function, for example via fusion with a bacterial albumin-binding domain (ABD) from *Streptococcal* protein G (Makrides *et al.*, 1996) or with a peptide selected against HSA from a phage display library (Dennis *et al.*, 2002; Nguyen *et al.*, 2006).

Second, a fundamentally different methodology for prolonging the plasma half-life of biopharmaceuticals is the conjugation with highly solvated and physiologically inert chemical polymers, thus effectively enlarging the hydrodynamic diameter of the therapeutic protein beyond the glomerular pore size of 3–5 nm (Caliceti and Veronese, 2003). Covalent coupling under biochemically mild conditions with activated derivatives of polyethylene glycol (PEG), either randomly via Lys side chains (Clark *et al.*, 1996) or by means of specifically introduced Cys residues (Rosendahl *et al.*, 2005), has been tremendously successful in yielding several approved drugs. Corresponding advantages have been achieved especially in conjunction with small proteins possessing specific pharmacological activity, for example Pegasys®, a chemically PEGylated recombinant IFN-α-2a (Harris and Chess, 2003; Walsh, 2003).

Many PEG derivatives, covering a range of sizes and including branched versions, with differing reactive groups and spacers, are currently available, thus making PEGylation the method of choice for tailoring the plasma half-life of biopharmaceuticals in the range from days to weeks. This offers advantages also for the clinical application of bacterially produced antibody fragments instead of costly full size Igs. Although the plasma half-life of an Fab' fragment is usually

shorter than 1 h, its area under the curve (AUC) can be dramatically increased 13.5-fold by site-specific conjugation with a single 40 kDa PEG chain (Chapman, 2002).

Unfortunately, the chemical coupling of a biologically active protein with synthetic polymers has drawbacks with respect to biopharmaceutical development and production. Suitable PEG derivatives are expensive, especially as high purity is needed, and their conjugation with a recombinant protein requires additional *in vitro* processing and purification steps, which lower the yield and raise the manufacturing costs, in particular under conditions of good manufacturing practice (GMP). Furthermore, the pharmaceutical function of a therapeutic protein may be hampered if amino-acid side chains in the vicinity of its biochemical active site become modified by the PEGylation process.

Apart from some peculiar mechanisms, the half-life-extending effect of PEG and related chemical polymers is mostly due to their nature as macromolecules with random conformational properties in aqueous solution and the associated large hydrodynamic volume (Caliceti and Veronese, 2003). On the basis of this notion, we investigated the possibility of using a structurally disordered biological homo-polymer of amino acids to achieve a similar effect. Poly-glycine is generally presumed as a polypeptide with random coil conformation in physiological solution (Shental-Bechor *et al.*, 2005) and offers the advantage that it may be directly incorporated into the recombinant protein drug by way of genetic fusion. Here, we describe the preparation of such fusion proteins with glycine-rich homo-amino-acid polymers (HAPs) using a recombinant Fab fragment of the clinically approved anti-HER2 (ErbB2) antibody trastuzumab (Herceptin®) (Perry and Wiseman, 1999), and we investigate their biophysical properties and the effects on the *in vivo* half-life in mice.

Materials and methods

Gene synthesis for the HAP

Recombinant DNA manipulation was performed according to general procedures (Sambrook *et al.*, 1989). Gene fragments encoding repetitive $(Gly_4Ser)_n$ sequences were obtained by hybridization and ligation of the two complementary oligodeoxynucleotides shown in Fig. 1 using concatamer formation in a directed manner via their mutually compatible but non-palindromic sticky ends. Oligodeoxynucleotides were purchased from IBA (Göttingen, Germany) and purified by preparative urea polyacrylamide gel electrophoresis (PAGE). Enzymatic phosphorylation was performed by mixing 200 pmol of both oligodeoxynucleotides in 100 µl 50 mM Tris–HCl pH 7.6, 10 mM $MgCl_2$, 5 mM DTT, 1 mM ATP and incubation for 30 min at 37°C in the presence of 10 U polynucleotide kinase (MBI Fermentas, St Leon-Rot, Germany). After denaturation for 10 min at 80°C, the mixture was cooled to room temperature overnight to achieve hybridization. Then 50 µl of this solution was ligated by adding 1 U T4 DNA ligase (MBI Fermentas) and 10 µl 100 mM Tris–HCl pH 7.4, 50 mM $MgCl_2$, 20 mM DTT, 10 mM ATP, 5 mM of each dATP, dCTP, dGTP and dTTP in a total volume of 100 µl and incubation for 15 min on ice. After 10 min heat inactivation at 70°C, the ligation products were separated by 1% (w/v) agarose gel electrophoresis in the presence of TAE buffer (40 mM Tris, 20 mM acetic acid and 1 mM EDTA) and 1 µg ml^{-1} ethidium bromide and bands corresponding to the assembled gene segments of desired lengths (Fig. 1B) were excised and isolated using phenol extraction. For cloning of the resulting synthetic gene fragments, a derivative of pASK75 (Skerra, 1994a), harboring the cDNA for a variant of neutrophil gelatinase-associated lipocalin (Breustedt *et al.*, 2006) fused with the C-terminal *Strep*-tag II (Skerra and Schmidt, 2000) and an *Eco*O109I restriction site in between (cf. Fig. 1C), was employed. This vector was cut with *Eco*O109I, dephosphorylated with alkaline phosphatase from shrimp (USB, Cleveland, OH, USA) and ligated with the synthetic DNA fragment from above. After transformation of *Escherichia coli* XL1-Blue (Bullock *et al.*, 1987), plasmids were prepared and the cloned inserts were characterized by restriction analysis and automated double-stranded DNA sequencing (ABI-Prism™310 Genetic analyzer, Perkin-Elmer Applied Biosystems, Weiterstadt, Germany)

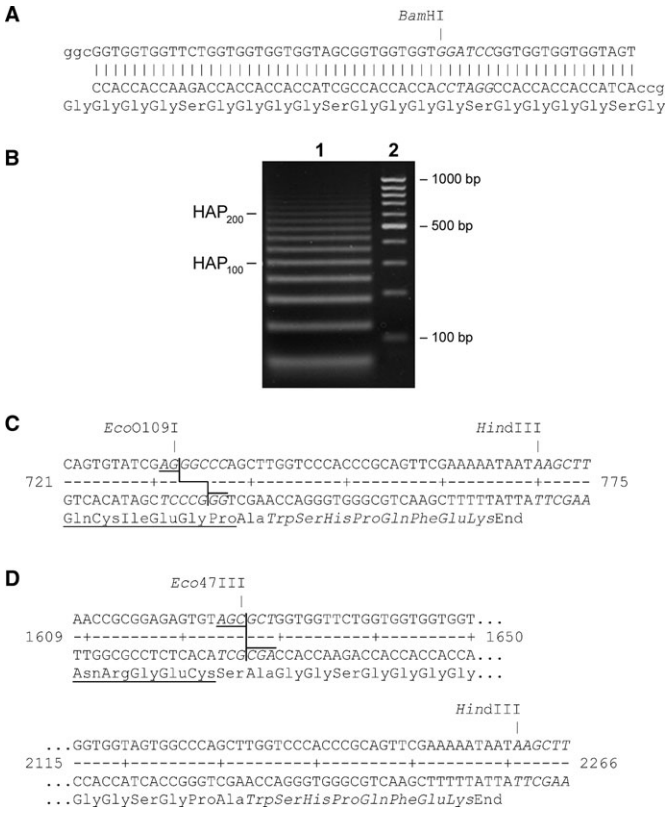

Fig. 1. Gene design and cloning strategy for glycine-rich HAP sequences. (**A**) Nucleotide and encoded amino-acid sequence of a building block obtained by hybridization of two complementary oligodeoxynucleotides, with two sticky ends (lower case letters) that are compatible with *Eco*O109I restriction sites. (**B**) Analysis of the building block by 1% agarose gel electrophoresis after phosphorylation and incomplete ligation. DNA bands were stained with ethidium bromide. (**C**) Nucleotide and encoded amino-acid sequence of the C-terminus (underlined) of a variant of human neutrophil gelatinase-associated lipocalin carrying the *Strep*-tag II (amino-acid sequence in italics) cloned on a pASK75 derivative (Breustedt *et al.*, 2006). An *Eco*O109I restriction site was introduced at the junction of both coding regions, leading to protruding ends compatible with the synthetic gene cassette after digest (indicated by bars). (**D**) Nucleotide and encoded amino-acid sequence of the C-terminus of the light chain of the 4D5 Fab fragment after insertion of the HAP sequence, followed by the *Strep*-tag II (italics). The unique *Eco*47III (blunt end after restriction digest indicated by bars) and *Hin*dIII restriction sites that were used for subcloning of the assembled HAP gene cassette are labeled (recognition sequences are shown in italics).

Table 1. Oligodeoxynucleotides for the assembly of the 4D5v8 V_H and V_L genes

Name	Nucleotide sequence
V_Hx	5′-GAA GTT CAA CTG CAG GAA TCC GGT GGT GGT CTG GTT CAG CCA GGT GGT TCC CTG-3′
V_Hy	5′-GGA GGA AAC GGT GAC CAG GGT ACC GTG ACC CCA GTA GTC CAT AGC GTA GAA ACC G-3′
V_Ha	5′-CAG CCA GGT GGT TCC CTG CGG CTC TCG TGT GCT GCT TCC GGT TTC AAC ATC AAA GAC ACC TAC ATC CAC TGG GTT CGT CAG G-3′
V_Hb	5′-GAA TCG GCA TAC CTG GTG TAA CCG TTG GTC GGG TAG ATA CGA GCA ACC CAT TCC AGG CCT TTA CCC GGA GCC TGA CGA ACC CAG TGA G-3′
V_Hc	5′-ACA CCA GGT ATG CCG ATT CAG TTA AAG GTC GTT TCA CCA TCT CGG CCG ACA CTT CCA AAA ACA CCG CTT ACC TCC AGA TGA ACT CCC TGC-3′
V_Hd	5′-AGT CGA TAG CGT AGA AAC CCT CAC CAC CCC AAC GGG AGC AAT AAT AAA CAG CTG TGT CTT CAG CAC GCA GGG AGT TCA TCT GGA G-3′
V_Lx	5′-GAC ATC GAG CTC ACC CAA TCC CCG TCC TCC CTG TCC GCT TCC GTT GGC GAC CGT GTT-3′
V_Ly	5′-TTT GAT CTC GAG TTT GGT ACC CTG ACC GAA GGT CGG CGG GGT GGT GTA GTG-3′
V_La	5′-TCC GTT GGC GAC CGT GTT ACC ATC ACG TGT AGG GCC TCG CAA GAC GTA AAC ACC GCC GTA GCG TGG TAT CAG CAG AAA CC-3′
V_Lb	5′-CGG AAC TCC GGA ATA CAG GAA GGA AGC GCT ATA GAT CAG CAG TTT CGG AGC TTT CCC GGG TTT CTG CTG ATA CCA CG-3′
V_Lc	5′-CCT GTA TTC CGG AGT TCC GAG CAG GTT CAG TGG TTC CCG TTC CGG TAC CGA CTT CAC CCT GAC GAT ATC CTC CCT-3′
V_Ld	5′-CGG CGG GGT GGT GTA GTG CTG TTG ACA GTA GTA GGT AGC GAA GTC TTC CGG CTG GAG GGA GGA TAT CGT CAG G-3′

using the BigDye™ terminator kit and oligodeoxynucleotide primers that enabled sequencing from both sides.

Construction of pASK88-4D5

The V_H and V_L domains of the humanized antibody 4D5v8 (Carter *et al.*, 1992b) were each assembled via polymerase chain reaction (PCR) from six partially overlapping oligodeoxynucleotides (Table 1), V_Hx, V_Ha, V_Hb, V_Hc, V_Hd and V_Hy for the V_H gene and V_Lx, V_La, V_Lb, V_Lc, V_Ld and V_Ly for the V_L gene, following a published procedure (Schlapschy *et al.*, 2004). The unique amplification products were cut with *Pst*I/*Bst*EII (V_H) and *Sac*I/*Xho*I (V_L), respectively, and then separately inserted into pASK88, a vector for the bacterial secretion of Fab fragments with constant domains of the human IgG1/κ subclass (Schiweck and Skerra, 1995), that had been cut with the same restriction enzymes. After transformation of *E. coli* JM83 (Yanisch-Perron *et al.*, 1985) with the ligation mixture, plasmids carrying genes with a correct sequence for each chain, as confirmed by automated double-stranded DNA sequencing, were identified and the corresponding V_H and V_L genes were finally combined on the same plasmid utilizing the unique *Xba*I and *Nco*I restriction sites.

Construction of pASK106-4D5

The part of pASK88-4D5 coding for the heavy chain of the Fab fragment together with the V_L moiety of its light chain was excised via *Xba*I and *Xho*I (Skerra, 1994b) and ligated with the likewise cut vector pASK106 (König and Skerra, 1998; Fiedler *et al.*, 2002), which encodes the ABD of *Streptococcal* protein G at the C-terminus of the human Ig light chain and is otherwise compatible. After transformation of *E. coli* JM83, the plasmid pASK106-4D5 was obtained.

Construction of pASK88G100-4D5 and pASK88G200-4D5

For construction of these plasmids, first an *Eco*47III restriction site was introduced into pASK88-D1.3 (Skerra, 1994b; Schiweck and Skerra, 1995) at the 3′-end of the human C_κ gene, using the QuikChange® site-directed mutagenesis kit (Stratagene, La Jolla, CA, USA) and primers 5′-GAGCTTC AACCGCGGAGAGTGTAGCGCTTAAGCTTGACCTGTGA AGTG-3′ as well as 5′-CACTTCACAGGTCAAGCTTA AGCGCTACACTCTCCGCGGTTGAAGCTC-3′ (*Eco*47III restriction site underlined). Then, a three-fragment ligation was performed: the vector backbone including the genes for V_H, C_H and V_L was derived from pASK88-4D5 by restriction digest with *Xho*I and *Hin*dIII; the gene for C_κ was isolated from pASK88-D1.3(*Eco*47III) from above by cutting with *Xho*I and *Eco*47III; the DNA fragment encoding the 100 or 200 residue HAP sequence was generated via PCR from the pre-assembled synthetic genes cloned on the pASK75 derivative using the oligodeoxynucleotides 5′-CGACCA-GTGTATCGAGAGCGCTGGTGGTTCTGGTGG-3′ (annealing at the upstream end; *Eco*47III restriction site underlined) and 5′-CGCAGTAGCGGTAAACG-3′ (annealing downstream of the *Hin*dIII restriction site on pASK75), thus also including the region encoding the C-terminal *Strep*-tag II, and cut with *Eco*47III and *Hin*dIII (cf. Fig. 1D). After ligation and transformation of *E. coli* XL1-Blue, the plasmids pASK88G100-4D5 and pASK88G200-4D5 were obtained.

Recombinant protein production and purification

The conventional recombinant 4D5 Fab fragment (calculated mass: 48 004 Da), its fusion with the ABD (53 289 Da), its fusion with the 100 residue HAP (55 619 Da) and its fusion with the 200 residue HAP (61 925 Da) were produced at 22°C in *E. coli* JM83, harboring the expression plasmids pASK88-4D5, pASK106-4D5, pASK88G100-4D5 and pASK88G200-4D5, respectively, using 2 l LB cultures (Sambrook *et al.*, 1989) containing 100 mg l^{-1} ampicillin. In the case of the two HAPylated Fab fragments, the medium was supplemented with 1 g l^{-1} glycine. Induction of foreign gene expression was performed with anhydrotetracycline at $OD_{550} = 0.5$ overnight for the 200 residue HAPylated Fab fragment (typically resulting in $OD_{550} \approx 1.8$ at harvest) and for 3 h in the case of the other three versions (typically resulting in $OD_{550} \approx 1.1$ at harvest). Periplasmic extraction in the presence of 500 mM sucrose, 1 mM EDTA, 100 mM Tris–HCl pH 8.0 was performed as described and followed by purification via the His_6 tag fused to the C-terminus of

the heavy chain using Zn(II)-charged IDA sepharose (Skerra, 1994b; Schiweck and Skerra, 1995). In the case of the two HAPylated Fab fragments, another purification step was accomplished by means of the *Strep*-tag II at the C-terminus of the light chains using streptavidin affinity chromatography (Skerra and Schmidt, 2000).

Purified Fab fragments were concentrated by ultrafiltration using Amicon Ultra centrifugal filter devices (30 000 MWCO; 15 ml; Millipore, Billerica, MA, USA) to $\sim$1.5 mg ml^{-1} and applied to a PD-10 gel filtration column (Amersham Biosciences, Uppsala, Sweden) for buffer exchange prior to radioactive labeling and biophysical analysis.

SDS–PAGE was performed using a high molarity Tris buffer system (Fling and Gregerson, 1986). Protein concentrations were determined according to their absorption at 280 nm using calculated extinction coefficients (Gill and von Hippel, 1989) of 68 290 M^{-1} cm^{-1} for the conventional 4D5 Fab fragment, 72 130 M^{-1} cm^{-1} for its ABD fusion, 73 980 M^{-1} cm^{-1} for its fusion with the 100 residue HAP and 73 980 M^{-1} cm^{-1} for its fusion with the 200 residue HAP. Reported yields of purified protein (mg l^{-1} OD^{-1}) were normalized to 1 l of bacterial culture and an optical density at harvest of 1.0.

Analytical gel filtration

Gel permeation chromatography (GPC) was carried out on a Superdex 75 HR 10/300 GL column (Amersham Biosciences) at a flow rate of 0.5 ml min^{-1} using an Äkta Purifier 10 system (Amersham Biosciences) with PBS (115 mM NaCl, 4 mM KH_2PO_4 and 16 mM Na_2HPO_4 pH 7.4) as running buffer. The purified Fab fragments (250 µl) were applied at a concentration of 0.5 mg ml^{-1}.

Circular dichroism spectroscopy

Secondary structure was analyzed using a J-810 spectropolarimeter (Jasco, Groß-Umstadt, Germany) equipped with a quartz cuvette 106-QS (0.1 mm path length; Hellma, Müllheim, Germany). Spectra were recorded from 190 to 250 nm at room temperature by accumulating 32 runs (bandwidth 1 nm, scan speed 100 nm min^{-1} and response 4 s) using 9–17 µM protein solutions in 50 mM K_2SO_4, 20 mM K-phosphate pH 7.5. After correction for solution blanks, spectra were smoothed using the instrument software, and the molar ellipticity Θ_M was calculated according to the equation

$$\Theta_M = \frac{\Theta_{obs}}{c\ d}$$

whereby Θ_{obs} denotes the measured ellipticity, c the protein concentration (mol l^{-1}), d the path length of the quartz cuvette (cm), and, finally, plotted against the wavelength using Kaleidagraph (Synergy Software, Reading, PA, USA).

Enzyme-linked immunosorbent assay for antigen-binding activity

96-well microtitre plates [12 × 8 well enzyme-linked immunosorbent assay (ELISA) strips with high binding capacity; Greiner, Frickenhausen, Germany] were coated for 1 h with 50 µl of the recombinant HER2/ErbB2 ectodomain (kindly provided by Tim Adams, CSIRO, Australia) at a concentration of 10 µg l^{-1} in 50 mM $NaHCO_3$ pH 9.6. The wells were blocked with 3% (w/v) bovine serum albumin (BSA) in PBS containing 0.1% (v/v) Tween-20 (PBS/T) for 1 h and washed three times with PBS/T. The anti-HER2 Fab fragments were applied in dilution series in PBS/T and incubated for 1 h. The wells were then washed three times with PBS/T and incubated for 1 h with 50 µl of a 1:1000 dilution in PBS/T of anti-human C_κ-light chain IgG alkaline phosphatase conjugate (DAKO, Glostrup, Denmark). After washing twice with PBS/T and twice with PBS, the enzymatic activity was detected using *p*-nitrophenyl phosphate as chromogenic substrate, and the data were fitted by non-linear least squares regression according to the law of mass action using KaleidaGraph software (Voss and Skerra, 1997).

Protein radioiodination

Prior to radioactive labeling, the 4D5 Fab fragment, its ABD fusion and the 100 as well as 200 residue HAP fusions were buffer-exchanged as appropriate (see below) and all four proteins were concentrated to 1 mg ml^{-1}. Radioiodination of the protein solutions was performed in Eppendorf tubes coated with Iodogen© (Pierce, Rockford, IL, USA). Coating was carried out by dissolving the required amount of Iodogen© in 150 µl dichloromethane, transferring the solution to an Eppendorf tube and gently evaporating the solvent via an argon stream under rotation. To each protein solution either $Na^{123}I$ (GE Healthcare, Buckinghamshire, UK) or $Na^{125}I$ (Hartmann Analytic, Brauschweig, Germany) in 0.05 M NaOH was added. After 15 min at room temperature, the reaction was stopped by removing the entire mixture from the insoluble oxidizing agent.

Using this procedure, 100 µg 4D5 Fab fragment in 100 µl 150 mM NaCl, 125 mM Tris–HCl pH 7.2 was radiolabeled with 64.4 MBq [^{123}I]iodide using 50 µg Iodogen©. About 200 µg Fab-Gly_{100} in 200 µl 150 mM NaCl, 125 mM Tris–HCl pH 7.2 was radiolabeled with 32.6 MBq [^{125}I]iodide using 150 µg Iodogen©. About 200 µg Fab-Gly_{200} in 200 µl 75 mM NaCl, 100 mM Tris–HCl pH 7.5 was radiolabeled with 115.8 MBq [^{123}I]iodide using 150 µg Iodogen©. About 100 µg Fab-ABD in 100 µl 150 mM NaCl, 125 mM Tris–HCl pH 7.2 was radiolabeled with 16.7 MBq [^{125}I]iodide using 50 µg Iodogen©. A second batch of radiolabeled Fab-ABD with higher specific activity was prepared using 100 µg Fab-ABD in 100 µl 150 mM NaCl, 125 mM Tris–HCl pH 7.2 as well as 50 µg Iodogen© and 74.0 MBq [^{125}I]iodide.

Quality control of the radioiodinated proteins was performed via size exclusion chromatography using a Sykam gradient system (Sykam GmbH, Fürstenfeldbruck, Germany) and an UVIS 200 photometer (Linear^{TM} Instruments Corporation, Reno, USA). For radioactivity measurement, the outlet of the photometer was connected to a Na(Tl) well-type scintillation counter Ace MateTM 925-Scint (EG&G Ortec, München, Germany). A Bio-Sil 250 Guard pre-column was connected to a Bio-Select 125 column (300 × 7.8 mm) (Bio-Rad Laboratories GmbH, Munich, Germany). Proteins were eluted with PBS (Dulbecco's, w/o Ca^{2+}, Mg^{2+}, BioChrom, Berlin, Germany). After quality control, all protein solutions were diluted with PBS to the activity concentrations needed for the animal experiments.

To be able to quantify radioiodine incorporation into the different proteins and to assess the influence of radioiodination conditions on protein integrity, iodination of all proteins with non-radioactive [^{127}I]iodide was performed under otherwise identical conditions. The amount of cold iodide needed

to mimic radioiodination conditions was calculated using the specific activities of [^{125}I]iodide (2000 Ci mmol^{-1}) and [^{123}I]iodide (5000 Ci mmol^{-1}), respectively. The following amounts of a 25 μM K-iodide stock solution in water were added to each reaction vial: 13.9 μl for iodo-4D5-Fab, 17.5 μl for iodo-Fab-Gly$_{100}$, 25 μl for iodo-Fab-Gly$_{200}$, 9 μl for iodo-Fab-ABD with low specific activity and 40 μl for iodo-Fab-ABD with high specific activity. After 15 min at room temperature, the protein solutions were removed from the insoluble oxidizing agent, transferred to another vial, immediately frozen and stored at −70°C. Subsequent analysis by SDS–PAGE revealed the same composition as for the freshly purified non-labeled proteins (data not shown), indicating that the iodination procedure did not affect the integrity of all four versions of the recombinant 4D5 Fab fragment.

Animal experiments

Female BALB/c mice (6–8 weeks) (Charles River, Sulzfeld, Germany) were injected intravenously with the following radioiodinated 4D5 Fab fragments:

Mice in group I ($n = 10$) simultaneously received 4.4 MBq ^{123}I-labeled conventional 4D5 Fab fragment (ca. 8.3 μg protein) and 666 kBq ^{125}I-labeled Fab-Gly$_{100}$ (ca. 4.1 μg protein) in 100 μl PBS; mice in group II ($n = 10$) simultaneously received 666 MBq ^{125}I-labeled Fab-Gly$_{100}$ (ca. 4.1 μg protein) and 3.7 MBq ^{123}I-labeled Fab-Gly$_{200}$ (ca. 7.7 μg protein) in 100 μl PBS; mice in group III ($n = 10$) simultaneously received 3.7 MBq ^{123}I-labeled Fab-Gly$_{200}$ (ca. 7.7 μg protein) and 629 kBq ^{125}I-labeled Fab-ABD (ca. 4.5 μg protein) in 100 μl PBS; mice in group IV ($n = 10$) received just 2.8 MBq ^{125}I-labeled Fab-ABD (ca. 4.5 μg protein) in 100 μl PBS.

Mice in group I ($n = 1$ per time point) were sacrificed at 1, 2, 4, 5, 6, 18, 20, 25 and 26 h post-injection (p.i.), mice in groups II–IV ($n = 1$ per time point) were sacrificed at 1, 4, 6, 18, 22, 26, 30 (or 28), 32, 40 and 42 h p.i. All animals were dissected, blood samples were collected and the organs of interest were removed, weighed and counted in a γ counter (Wallach, Turku, Finland) using an energy resolving dual-isotope protocol with energy windows of 15–85 keV for ^{125}I and 135–172 keV for ^{123}I. Activity concentration in blood as well as activity accumulation in organs (liver, stomach, intestine, spleen, pancreas, kidney and muscle) were calculated in percent injected dose per gram blood or tissue (%ID g^{-1}).

To determine the plasma half-life of the 4D5 Fab fragment and its variants, the experimental activity data, $A(t)$, were plotted against time post-intravenous injection, t, and numerically fitted using KaleidaGraph software. A bi-exponential decline was assumed according to the equation

$$A(t) = A_\alpha e^{-(t \ln 2)/\tau^\alpha_{1/2}} + (A_0 - A_\alpha) e^{-(t \ln 2)/\tau^\beta_{1/2}}$$

whereby $\tau^\alpha_{1/2}$ and $\tau^\beta_{1/2}$ are the initial and terminal plasma half-life parameters, respectively, and A_α the activity amplitude for the α phase. A_0 is the total blood activity at time point zero, which should have a value of ca. 66% ID g^{-1} for mice under the assumption of an average animal weight of 25 g and a typical blood to body weight ratio of 0.06.

Results

Gene design for a glycine-rich HAP

Although, from a biophysical perspective, a homo-glycine polymer would probably constitute the most desirable fusion partner with a random coil structure under physiological buffer conditions, its preparation via recombinant DNA technology poses some practical challenges. First of all, Gly is encoded by a GGN triplet such that DNA regions that code for stretches of repeated Gly residues are extremely G/C-rich, which hampers cloning and sequencing. Necessarily, such coding regions bear high internal homology, which makes them prone to deletion *in vivo* by genetic recombination and related mechanisms or in the course of *in vitro* manipulation steps required for gene synthesis and cloning, including replication slippage (Viguera *et al.*, 2001) during PCR. The situation becomes even more difficult when taking into consideration that only GGC and GGT constitute preferred Gly codons in highly expressed *E. coli* genes, whereas GGG and especially GGA are known as 'rare' codons (Chen and Texada, 2006).

On one hand, in order to prevent poor translational efficiency because of premature exhaustion of charged tRNAs such rare codons should be avoided, whereas, on the other, a more diverse nucleic acid sequence would enhance the specificity of hybridization during gene assembly from synthetic oligodeoxynucleotides. To escape this dilemma, we decided to construct a mixed HAP containing 20% Ser residues with the repetitive sequence $(Gly_4Ser)_n$. Oligomers of the conformationally highly flexible Gly_4Ser motif are already in wide use to link separate domains in recombinant fusion proteins. For example, the $(Gly_4Ser)_3$ spacer is commonly employed for the preparation of single chain Fv fragments (Bird and Walker, 1991; Turner *et al.*, 1997; Hennecke *et al.*, 1998).

On the basis of this motif, we designed a gene cassette encoding four repetitive Gly_4Ser units (Fig. 1), whereby codons were chosen according to the following criteria: (i) four different Ser codons were used to avoid internal repeats longer than 12 or 13 nucleotides; (ii) GGT was predominantly employed as codon for Gly because it is one of the two preferred codons in *E. coli* genes and, in contrast to GGC, its choice helped to keep the G/C content of the synthetic gene in a moderate range of 65%; (iii) one rare GGA codon was used to introduce, in conjunction with a TCC codon for Ser, a diagnostic *Bam*HI restriction site approximately in the middle of each cassette and (iv) one GGC codon was used to create complementary sticky ends of three nucleotides with high base-pairing propensity on both sides of the gene cassette (Fig. 1A). Thus, after hybridization of two corresponding synthetic oligodeoxynucleotides, these two 5′-protruding but non-palindromic ends (because of the odd number of nucleotides) could be used for efficient unidirectional ligation.

The resulting ladder of defined ligation products was electrophoretically separated on an agarose gel (Sambrook *et al.*, 1989), each band corresponding to a gene differing by 20 encoded amino acids from its neighbor (Fig. 1B). Synthetic DNA fragments of the desired lengths were excised, eluted from the gel and subcloned on a vector via a unique *Eco*O109I restriction site, with the compatible recognition sequence AG′GCCC, such that only the coding orientation of the insert was possible and a continuous reading frame with the fused protein on the N-terminal side as well as the

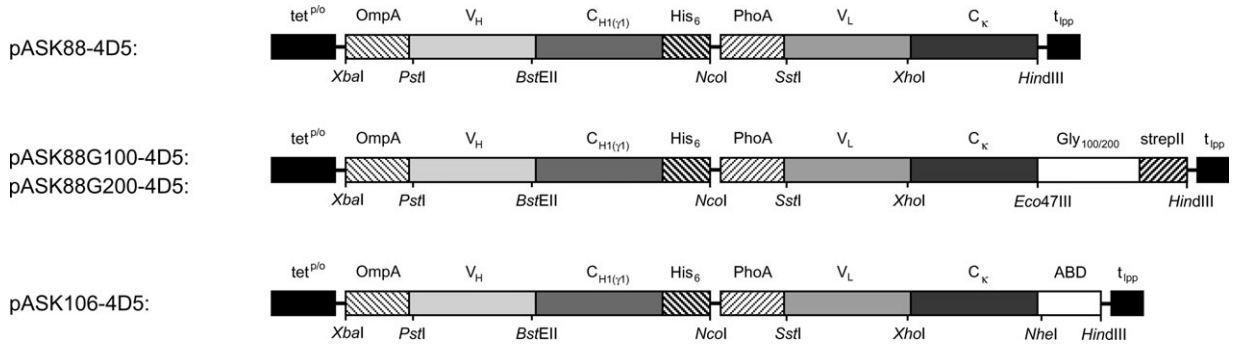

Fig. 2. Schematic representation of the expression cassette on the plasmids pASK88-4D5, pASK88G100-4D5, pASK88G200-4D5 and pASK106-4D5 for the conventional 4D5 Fab fragment, the two versions with HAP sequences of either 100 or 200 residues appended to the C-terminus of the light chain and the corresponding ABD fusion protein, respectively. The two structural genes for the heavy chain (comprising *Omp*A signal peptide, V_H domain, human C_H1 domain of subclass IgG1 as well as the His_6 tag) and for the light chain (comprising *Pho*A signal peptide, V_L domain, human C_κ domain and HAP_{100}, HAP_{200} or ABD) are arranged as a dicistronic operon under transcriptional control of the tetracycline promoter/operator ($tet^{p/o}$) and ending with the lipoprotein terminator (t_{lpp}). The plasmid backbone is identical with that of the generic cloning and expression vector pASK75 (Skerra, 1994a). Singular restriction sites are indicated.

Strep-tag II on the C-terminal side was obtained (Fig. 1C). In this way, gene cassettes coding for HAPs with 40, 60, 80, 100, 140 and 200 residues were successfully cloned in the *E. coli* K-12 strain XL1-Blue (Bullock *et al.*, 1987) and characterized by DNA sequencing. During propagation and further cloning steps, using either XL1-Blue or JM83 (Yanisch-Perron *et al.*, 1985) *E. coli* strains, no signs of deletion events or plasmid rearrangement were observed, indicating a high genetic stability of the designed coding region.

Construction and bacterial production of HAPylated anti-HER2 Fab fragments

To investigate the biophysical properties and effects on *in vivo* half-life of HAPs with different lengths, a recombinant Fab fragment of the humanized anti-HER2 antibody trastuzumab, initially described as 4D5-8 (Carter *et al.*, 1992b), was chosen. Trastuzumab/Herceptin® (Perry and Wiseman, 1999) has been approved for clinical treatment of HER2-overexpressing metastatic breast cancer and both the full size antibody as well as its bacterially produced Fab fragment (Carter *et al.*, 1992a) have been biochemically thoroughly characterized, including X-ray structural analysis of the Fv and Fab fragments (Eigenbrot *et al.*, 1993) and also of the complex between the Fab fragment and the extracellular region of the HER2 receptor (Cho *et al.*, 2003). Notably, an engineered version of the Fab fragment fused with an albumin-binding peptide, which exhibits increased plasma half-life, was recently described (Nguyen *et al.*, 2006). For the present study, we reconstituted the variable gene regions of the optimized version no. 8 of the humanized anti-HER2 antibody 4D5 via gene synthesis.

Following an earlier described strategy (Essen and Skerra, 1994), V_H and V_L were separately assembled via PCR from six partially overlapping oligodeoxynucleotides (Table I) representing the coding and non-coding strands in an alternating manner (see Materials and methods section) and subcloned using flanking restriction sites (Schlapschy *et al.*, 2004). After confirmation of the DNA sequences, V_H and V_L were together subcloned on the previously developed vector pASK88 for the bacterial secretion of recombinant Fab fragments (Schiweck and Skerra, 1995). pASK88 is an improved version of pASK19 (Plückthun and Skerra, 1989) which carries the tetracycline promoter/operator (Skerra, 1994a) instead of the $lac^{p/o}$ and provides already the constant region genes of the human IgG1/κ subclass (Fig. 2). Both chains of the encoded Fab fragment end with the Cys residues that give rise to the characteristic interchain disulfide bond of this subclass. In the case of the heavy chain, the Cys residue is followed by a His_6 tag (Skerra *et al.*, 1991; Skerra, 1994b) to allow purification via immobilized metal affinity chromatography (IMAC). Hence, apart from a few conservative amino-acid exchanges (V_H: Val5 → Gln; V_L: Gln3 → Glu, Met4 → Leu, Val104 → Leu), which were necessary to make use of the standardized restriction sites on pASK88, and the exchange of the truncated hinge region by the His_6 tag, the encoded Fab fragment on pASK88-4D5 is identical to the one that was described during the development of trastuzumab (Carter *et al.*, 1992a).

The C-terminus of the light chain of the cloned 4D5 Fab fragment was chosen for fusion with the HAP sequences. After introduction of an appropriate singular restriction site directly downstream of the C-terminal Cys residue of the structural gene for the C_κ domain, the gene cassettes encoding HAPs with 100 and with 200 residues, i.e. $(Gly_4Ser)_{20}$ and $(Gly_4Ser)_{40}$, together with a C-terminal sequence encoding the *Strep*-tag II (Skerra and Schmidt, 2000), were inserted, yielding the plasmids pASK88G100-4D5 and pASK88G200-4D5, respectively (Fig. 2). Furthermore, to allow comparison with the albumin carrier strategy for plasma half-life extension, a fusion between the 4D5 Fab fragment and an ABD from *Streptococcal* protein G (Åkerström *et al.*, 1987; Olsson *et al.*, 1987) was constructed. To this end, the structural genes for V_H and V_L were subcloned onto the previously described vector pASK106 (König and Skerra, 1998; Fiedler *et al.*, 2002), resulting in an analogous expression cassette for the 4D5 Fab fragment, i.e. carrying human constant domains and the His_6 tag at the C-terminus of the heavy chain, with the ABD fused to the C-terminus of the light chain (Fig. 2).

All four recombinant Fab fragments were secreted in *E. coli* (employing *Omp*A and *Pho*A bacterial signal sequences for the two Ig chains, respectively; cf. Fig. 2) and successfully purified from the periplasmic cell fraction via IMAC. In the case of the 100 and 200 residue HAP versions, the LB culture medium was supplemented with 1 g l^{-1}

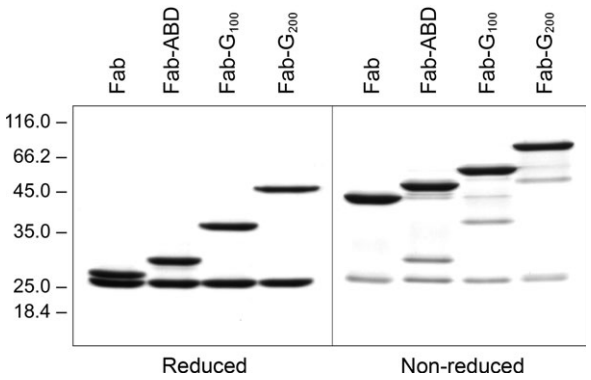

Fig. 3. Analysis of the purified recombinant 4D5 Fab fragment, its ABD fusion and its HAPylated versions with 100 or 200 residues, respectively, by 12% SDS–PAGE, followed by staining with Coomassie Brilliant Blue R-250. The gel shows 5 μg protein samples each of the conventional 4D5 Fab fragment, the Fab fragment fused with the ABD, the Fab fragment fused with the 100 residue HAP and the Fab fragment fused with the 200 residue HAP. Samples on the left side were reduced with 2-mercaptoethanol, whereas on the right side they were left unreduced. Sizes of protein markers (kDa)—applied under reducing conditions—are indicated on the left.

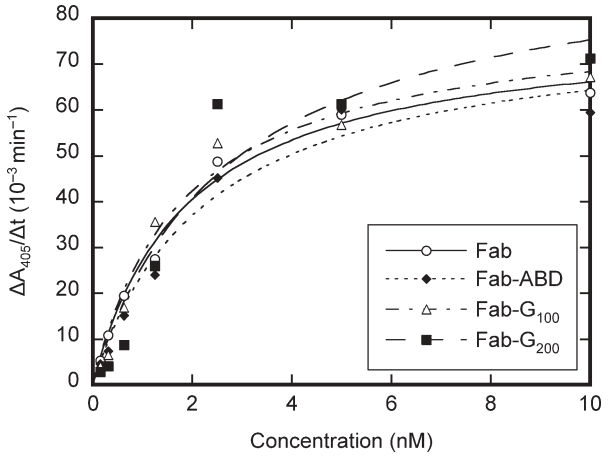

Fig. 4. Comparative analysis of the purified recombinant 4D5 Fab fragment, its ABD fusion and its HAPylated versions with 100 or 200 residues, respectively, by ELISA. The wells of a microtitre plate were coated with the recombinant HER2/ErbB2 ectodomain and the purified Fab fragments were applied in dilution series. Bound antibody fragment was detected with anti-human C_κ IgG alkaline phosphatase conjugate, followed by chromogenic reaction with *p*-nitrophenyl phosphate. No signal was detected with the secondary antibody conjugate alone (not shown).

glycine to avoid metabolic deprivation, resulting from the enhanced uptake of this amino acid into the biosynthetic fusion proteins. Supplementation of Gly had no effect on bacterial cell growth or viability. However, protein yields increased by a factor of two and four for the 100 and 200 residue HAP versions, respectively, compared with the situation without added Gly. Furthermore, prolongation of the induction time up to 12 h in the case of the 200 residue HAP increased the protein yield by another factor of two when compared with the 3 h induction period that was used for the other three Fab fragments.

In the case of the conventional 4D5 Fab fragment and its ABD fusion, homogeneous protein preparations were obtained after the one-step IMAC purification (Fig. 3), with yields of 0.5 mg l^{-1} OD^{-1} and 0.3 mg l^{-1} OD^{-1}, respectively. However, for the two HAPylated Fab fragments an excess of the heavy chain was detected in the protein fractions obtained after IMAC, indicating some hindrance in the association between light and heavy chains, which was more pronounced for the 200 amino-acid polymer tail. To ensure stoichiometric composition of the two Ig chains, a second affinity purification was applied, utilizing the *Strep*-tag II that was fused to the C-termini of both HAP sequences. After this additional step, both the 100 and 200 residue HAP versions of the 4D5 Fab fragment were obtained as homogeneous preparations (Fig. 3), with yields of 0.25 mg l^{-1} OD^{-1} and 0.2 mg l^{-1} OD^{-1}, respectively.

The 100 residue HAP version was fully stable in 150 mM NaCl, 125 mM Tris–HCl pH 7.2 at concentrations up to 1.5 mg ml^{-1} for several weeks. In contrast, the 200 residue version showed some tendency to aggregate during storage at 4°C in different buffers like PBS or streptavidin affinity chromatography buffer (150 mM NaCl, 1 mM EDTA, 100 mM Tris–HCl pH 8.0), in particular after concentration by ultrafiltration. Nevertheless, shock freezing in liquid nitrogen enabled prolonged storage at −80°C in 75 mM NaCl, 100 mM Tris–HCl pH 7.5 without significant signs of protein aggregation after thawing.

The influence of the HAP fusion on the antigen-binding activity of the 4D5 Fab fragment was tested in an ELISA using the recombinant HER2/ErbB2 ectodomain (Garrett *et al.*, 2003) as antigen. The 4D5 Fab fragment as well as its HAP and also ABD fusion variants gave rise to pronounced binding signals with typical saturation curves, showing no significant difference in the half-maximal concentration values as a measure for their antigen affinities (Fig. 4).

Biophysical characterization of HAPylated anti-HER2 Fab fragments

Analysis of the recombinant Fab fragments via SDS–PAGE under non-reducing conditions indicated the proper formation of the interchain disulfide bond for the conventional format as well as for the three fusion proteins, with at least 90% covalent linkage in all cases (Fig. 3). Mass-spectrometric analysis confirmed, in each case, the expected molecular weight: 48 004 *m/z* for the unfused 4D5 Fab fragment (calculated: 48 004 g mol^{-1}); 55 620 *m/z* for the 100 residue HAP fusion (calculated: 55 619 g mol^{-1}); 61 927 *m/z* for the 200 residue HAP fusion (calculated: 61 925 g mol^{-1}) and 53 289 *m/z* for the ABD fusion (calculated: 53 289 g mol^{-1}). Thus, there was no indication of prematurely terminated gene products, which might have been expected for the HAPylated proteins, albeit these should have been largely lost during the *Strep*-tag purification, if present at all.

Analytical gel filtration on a calibrated Superdex S75 10/300 GL column resulted in a single homogeneous peak for each of the four Fab fragments (Fig. 5), whereby the elution volume decreased in the order: unfused 4D5 Fab fragment, ABD fusion, HAP 100 fusion and HAP 200 fusion, with deduced molecular weights corresponding to ca. 35, 40, 58 and 77 kDa, respectively. Thus, the apparent molecular weight of the conventional Fab fragment was by 27% lower than its true mass. This phenomenon has been observed for other Fab fragments as well and may be explained by the extended tertiary structure of this protein, which considerably differs from the ideal spherical shape that forms the basis for molecular weight calculations from gel permeation chromatography (Andrews, 1964). Interestingly, the HAP 100

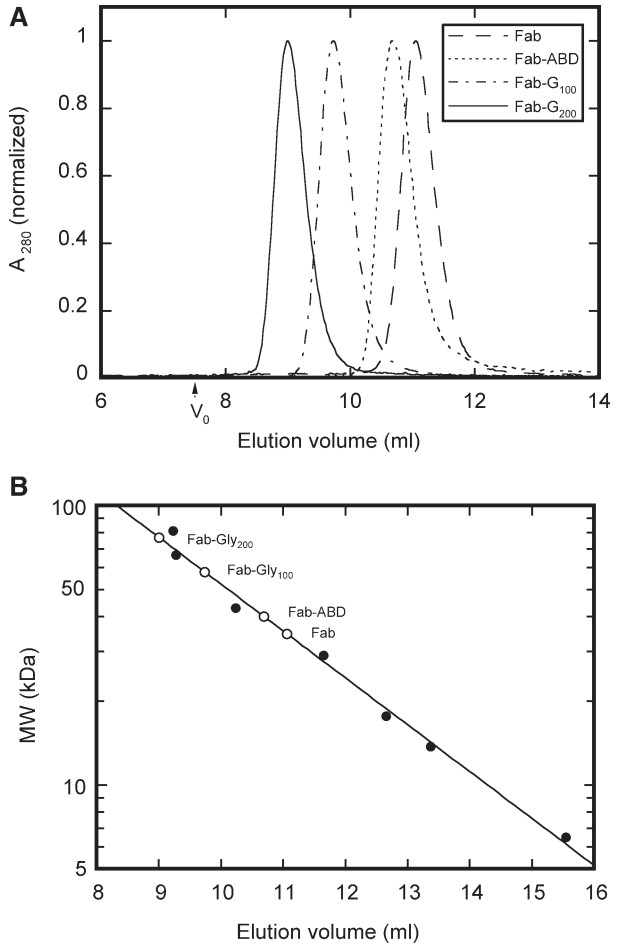

Fig. 5. Quantitative analysis of the hydrodynamic volumes of the purified recombinant 4D5 Fab fragment, its ABD fusion and its HAPylated versions with 100 or 200 residues. (**A**) Analytical gel permeation chromatography. About 250 μl of each protein at a concentration of 0.5 mg ml^{-1} was applied to a Superdex S75 10/300 GL column equilibrated with PBS buffer. Maximal absorption at 280 nm of each chromatography run was normalized to 1. The arrow indicates the exclusion volume of the column (7.5 ml). (**B**) Calibration curve for the chromatograms from (A). The logarithm of the molecular weights (MWs) of marker proteins (aprotinin, 6.5 kDa; ribonuclease, 13.7 kDa; myoglobin, 17.6 kDa; carbonic anhydrase, 29.0 kDa; ovalbumin, 43.0 kDa; BSA, 66.3 kDa and transferrin, 81.0 kDa) was plotted versus their elution volumes (black circles) and fitted by a straight line. From the observed elution volumes of the 4D5 Fab fragment and its fusion variants (hollow circles), their apparent molecular weights were deduced (see text).

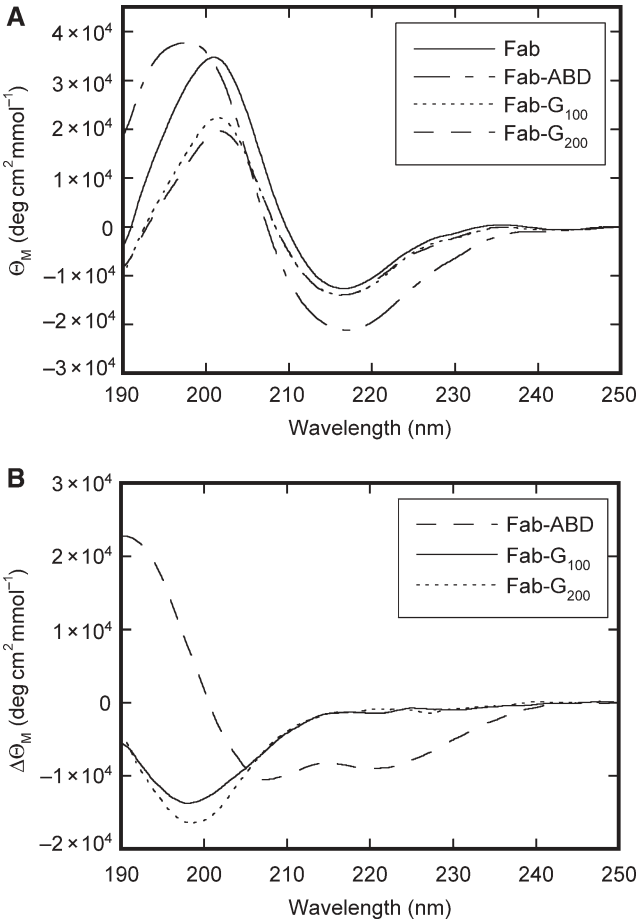

Fig. 6. Secondary structure analysis by CD spectroscopy. (**A**) CD spectra of the purified recombinant 4D5 Fab fragment, its ABD fusion and its HAPylated versions with 100 or 200 residues. Spectra were recorded at room temperature in 50 mM K_2SO_4, 20 mM K-phosphate pH 7.5 using a 0.01 cm quartz cuvette and normalized to the molar ellipticity, Θ_M, for each protein. (**B**) Molar difference CD spectra for the ABD fusion and the HAPylated versions with 100 or 200 residues obtained by subtraction of the spectrum for the unfused Fab fragment.

version and, even more pronounced, the HAP 200 version showed significantly higher apparent molecular weights in this experiment. In the case of the 200 residue HAP fusion protein, the size increase was 24% compared with the true mass, which corresponds to an increase by 120% compared with the factual elution behavior of the unfused Fab fragment. This observation clearly indicates the effect of an enhanced hydrodynamic volume that is to be expected if the HAP assumes a random coil structure (Squire, 1981).

To gain further information about the conformational properties of the fusion moiety, circular dichroism (CD) spectra were recorded for the four recombinant Fab fragments (Fig. 6). The CD spectrum for the conventional 4D5 Fab fragment had the typical appearance of a predominant β-sheet protein, with a broad negative maximum ~216 nm and a positive band near 200 nm (Greenfield and Fasman, 1969; Sreerama and Woody, 2000; Fändrich and Dobson, 2002). However, the spectra of the three fusion proteins revealed characteristic deviations. To analyze the spectroscopic contributions by each fusion partner in greater detail, we calculated the molar difference CD spectra with respect to the unfused Fab fragment.

Indeed, the difference CD spectrum for the ABD fusion exhibited the double minimum at 208 and 222 nm that is characteristic for α-helical secondary structure (Greenfield and Fasman, 1969; Sreerama and Woody, 2000; Fändrich and Dobson, 2002) and in nice agreement with the three-helix bundle structure of this domain known from its biomolecular NMR analysis (Kraulis *et al.*, 1996). In contrast, in the case of the 100 and 200 residue HAP fusions, a strong minimum at 198 nm was observed in the difference CD spectrum, which is indicative of random coil conformation (Greenfield and Fasman, 1969; Sreerama and Woody, 2000; Fändrich and Dobson, 2002). Notably, since Gly is an achiral amino acid and itself shows no CD signal, this spectroscopic effect must be mostly due to the Ser residues that were introduced into the polymer sequence. When considered on a molar basis, the amplitude at 198 nm of the 200 residue HAP was larger than the amplitude of the 100 residue fusion, which

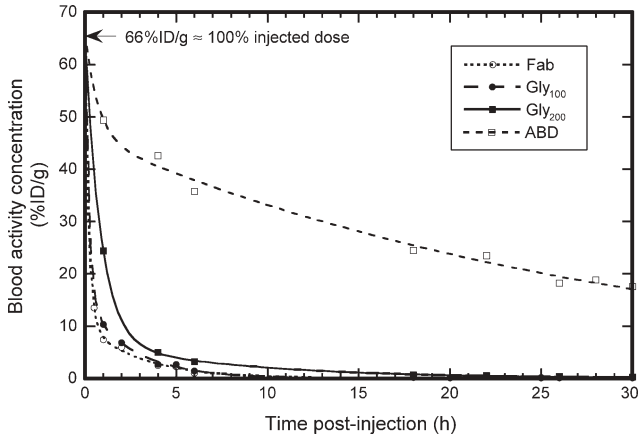

Fig. 7. Pharmacokinetics of the radioiodinated recombinant 4D5 Fab fragment, its ABD fusion and its HAPylated versions with 100 or 200 residues, respectively, in the blood of BALB/c mice up to 30 h post-intravenous injection. The conventional Fab fragment and also both HAP fusion proteins clearly show bi-exponential decay. Hence, all data series were numerically evaluated according to a two-compartment model (Mahmood, 2006). Curve fit revealed initial half-lives of 0.14 ± 0.01 h, 0.15 ± 0.05 h, 0.59 ± 0.01 h and 0.49 ± 0.15 h for the 4D5 Fab fragment, its HAPylated versions with 100 or 200 residues and its ABD fusion, respectively, whereas the corresponding terminal half-lives were 2.1 ± 0.2 h, 1.9 ± 0.2 h, 5.7 ± 0.5 h and 20.9 ± 1.5 h.

reveals that the $(Gly_4Ser)_n$ sequence as part of the recombinant fusion protein represents a random coil polymer under physiological buffer conditions in a nearly quantitative manner.

Pharmacokinetic analysis of HAPylated anti-HER2 Fab fragments

The plasma half-life of the HAPylated Fab fragments was compared with the conventional recombinant 4D5 Fab fragment as well as its ABD fusion in BALB/c mice using radioiodinated protein samples (Fig. 7). The protein preparations were either labeled with [^{123}I]iodide or with [^{125}I]iodide and always a mixture of two samples was applied. The two radiolabels were independently quantified by γ-detection in suitable energy windows, i.e. 15–85 keV for ^{125}I and 135–172 keV for ^{123}I, thus allowing the side by side comparison of two different proteins in the same animal and avoiding methodological errors due to possible *in vivo* dehalogenation and/or metabolization of the radioactive iodine (Ferl *et al.*, 2006).

As determined by size exclusion chromatography, the efficiency of radioiodide incorporation and radiochemical purity was >96% for the different versions of the 4D5 Fab fragment investigated. In all analytical quality control chromatograms, the radioiodinated protein co-eluted with the unlabeled precursor, and no further peaks were detectable both via UV absorption at 220 nm and in the radioactivity profile, indicating full integrity of the radiolabeled proteins, without signs of protein aggregation or degradation. This was consistent with an SDS–PAGE analysis of reference protein samples, which were labeled with non-radioactive iodide under identical conditions and also showed no signs of decomposition.

When measuring the kinetics of blood clearance and tissue distribution *in vivo* (Fig. 7), the conventional recombinant 4D5 Fab fragment and both of its HAP fusion proteins clearly showed bi-exponential decline, whereby the unfused Fab fragment exhibited the fastest excretion of the protein samples tested. The distribution phase was always quick, with half-life values between 0.1 and 0.6 h. The terminal half-life of ~2 h both for the unfused Fab fragment and for its 100 residue HAP version was also rather short and mutually identical within experimental error. This number is in agreement with the value of 1.28 h described for the unfused anti-HER2 Fab fragment by others (Nguyen *et al.*, 2006).

In contrast, the elimination phase of the 200 residue HAP version of the 4D5 Fab fragment was significantly slower, with a terminal half-life of 5.7 ± 0.5 h, indicating prolonged circulation by a factor of almost three. On the other hand, the longest terminal half-life of 20.9 ± 1.5 h was observed for the ADB fusion protein, which was tested for comparison. This number is essentially identical with the terminal half-life described for the recombinant anti-HER2 Fab fragment that carries a peptide tag with HSA-binding activity (Nguyen *et al.*, 2006).

Similar uptake (clearance) kinetics was measured for intestine, pancreas, lung, spleen and muscle (not shown). Tracer uptake in the liver was generally low, reaching liver/blood ratios of 0.4 to 0.5 for the unfused 4D5 Fab fragment and 0.3 to 0.4 for both HAPylated versions within the first 6 h. Compared with the ABD fusion protein, the other recombinant Fab fragments were apparently faster excreted via the kidneys, thus leading to a somewhat higher initial uptake in this organ.

Discussion

In this study, we have successfully prepared fusion proteins of an Fab fragment having therapeutically relevant antigen specificity with HAPs of up to 200 residues. The choice of the glycine-rich polymer sequence, with 20% Ser content, was governed by the expected high entropy as well as low tendency to form intermolecular interactions due to the lack of functional side chains, except for the solvated alcohol groups of the Ser residues, and conformational disorder of the polypeptide backbone. Sequences of this kind should be biologically inert, especially with respect to proteolysis, immunogenicity, neutral pI, binding to cell surface receptors as well as internalization, but still biodegradable, contrasting with synthetic polymers such as PEG.

Similar repetitive amino-acid sequences, although with shorter lengths, exist in nature. For example, in the minor coat protein g3p of filamentous bacteriophages, multiple copies of a Gly_3Ser spacer—plus some interspersed Glu residues—link in particular its N2 and CT domains in a flexible manner (Beck and Zink, 1981) and this polypeptide stretch obviously resists the harsh conditions in the mammalian gut system. Even human proteins with similar sequences exist, e.g. zinc finger DNA-binding protein 99 (GenBank: AF125158) and mitogen-activated protein kinase kinase 4 (GenBank:CR536564), hence the risk of an immunogenic side effect should be low. In fact, various versions of single-chain Fv fragments of antibodies, wherein the two variable domains are covalently connected by a $(Gly_4Ser)_3$ linker, are already subject to clinical trials (Holliger and Hudson, 2005).

Using an appropriate gene design, the synthesis of the coding region for multiple repeats of the Gly_4Ser amino-acid sequence, which is composed of 60 bp repetitive units on the DNA level and involves a high content of G/C base pairs, was possible without major obstacles. We succeeded to clone these sequences and to propagate plasmids with error-free inserts in standard *E. coli* strains without signs of

recombination or genetic instability. Thus, from this perspective, it should be feasible to generate coding regions for even longer HAP sequences.

The production of the corresponding fusion proteins via secretion into the bacterial periplasm, which is necessary to ensure disulfide bond formation and proper folding of the recombinant antibody fragment (Plückthun and Skerra, 1989), was possible both for the 100 and 200 residue HAP fusions with yields of 40–50% (at the shake flask scale and up to now without further optimization) compared with the conventional Fab fragment. However, the efficient biosynthesis of the 200 residue HAP fusion protein required special conditions, i.e. the addition of glycine to the culture medium and a longer induction time for gene expression, because otherwise the yields were significantly diminished. This effect is probably due to increasing deprivation of Gly-charged tRNAs during protein synthesis with growing length of the biopolymer and is likely to limit the production of much longer sequences of this kind using ordinary strains of *E. coli*.

Whereas plasmids for overexpression of various tRNAs have been described in conjunction with the expression of cDNAs containing rare codons in *E. coli* (Del Tito *et al.*, 1995; Dieci *et al.*, 2000; Novy *et al.*, 2001), corresponding vectors for more abundant tRNAs are not generally available. Nevertheless, it should be feasible to overexpress tRNAs recognizing GGT and GGC codons (Chen and Texada, 2006) for Gly (i.e. *gly*W or the operon *gly*VXY) and also the cognate glycyl-tRNA synthetase, possibly together with corresponding genes for Ser, in order to achieve the production of even longer HAP sequences with acceptable yields, especially if combined with optimized industrial strains and bacterial high density fermentation.

Both the 100 and the 200 residue HAP fusion proteins could be purified as homogeneous preparations using two-step affinity chromatography via the His_6 tag fused to the heavy chain and the *Strep*-tag II fused to the C-terminus of the correspondingly extended light chain. Usually, the purification of a recombinant Fab fragment is possible just using one tag fused to its heavy chain. As this subunit alone is insoluble and not able to form a stable homo-dimer in most cases, the heterodimer with the light chain is selectively isolated under these conditions (Skerra, 1994b). However, it had to be noted for both HAP fusion proteins that preparations with non-stoichiometric chain composition were obtained after this first purification step, in contrast with the unfused 4D5 Fab fragment or its ABD fusion protein.

Albeit the presence of the HAP fusion moiety with its large hydrodynamic volume might hamper the association between light and heavy chain of the Fab fragment, it is not clear why an excess of the unfused heavy chain was isolated during IMAC in this case. Nevertheless, a second mild purification step employing the *Strep*-tag II (Skerra and Schmidt, 2000) appended to the C-terminus of the light chain, downstream of the HAP sequence, resulted in homogeneous protein preparations, with almost quantitative formation of the interchain disulfide bond as confirmed by SDS–PAGE and mass spectrometry. Thus, it can be assumed that Fab fragments with even longer HAP sequences may be obtained in this way.

These preparations showed essentially identical antigen-binding activity with the unfused recombinant 4D5 Fab fragment, which was demonstrated by ELISA using the HER2/ErbB2 ectodomain as antigen. Insofar, fusion with the HAP sequences did not affect the functionality of the Fab fragment. Unfortunately, however, it was observed that the 200 residue HAPylated protein showed a pronounced aggregation tendency, which was also detectable, although less evident, for the 100 residue HAP version. This finding is in agreement with early accounts of poor solubility for chemically synthesized polymers of glycine (Bamford *et al.*, 1956) and, apparently, the introduction of 20% Ser residues with their polar hydroxyl groups in the present instance did not sufficiently alleviate this problem.

Even though it was possible to control the aggregation behavior by choosing appropriate buffer conditions, it has to be anticipated that this feature will probably limit the length of practically useful HAP sequences based on the Gly_4Ser repetitive unit. Yet, with the aim to obtain a true random chain, similar to PEG, Gly offers the most attractive features. Whereas homo-polymers of most amino acids, in particular the hydrophobic ones, are usually insoluble in aqueous solution (Bamford *et al.*, 1956), homo-polymers of several hydrophilic amino acids are known to form secondary structures, for example α-helix in the case of Ala (Shental-Bechor *et al.*, 2005) and β-sheet in the case of Ser (Quadrifoglio and Urry, 1968). Charged amino acids also tend to adopt regular structures, but this might still be acceptable if the resulting hydrodynamic radius is large enough, in particular for anionic polymers, which also tend to retard filtration via the kidney (Colcher *et al.*, 1998; Caliceti and Veronese, 2003). Nevertheless, non-specific adsorption to cell surfaces and extracellular matrix probably prevents the general use of such sequences so that a more inert HAP, like the one investigated here, should be desirable.

Due to the lack of a side chain and its nature as the only achiral amino acid, Gly is known to be the most flexible amino acid (Schulz and Schirmer, 1979; Creighton, 1993) and hence, it is generally assumed to adopt a random coil conformation (Shental-Bechor *et al.*, 2005) with a large solution entropy and low tendency to participate in intermolecular interactions. However, although numerous theoretical calculations of the conformational properties of its random-coil chain (under denaturing conditions) have been described (Cantor and Schimmel, 1980), starting with the early work of Flory and coworkers (Brant *et al.*, 1967), surprisingly few experimental data exist for its conformational state under physiological buffer conditions, i.e. in the absence of denaturants and at ambient temperature.

A CD analysis has been described for poly(Ala-Gly-Gly) (Rippon and Walton, 1971), wherein a poly-glycine II conformation similar to the collagen triple helix was detected in aqueous solution. However, this conformation could have been induced by the periodic trimer sequence and is probably not a valid model for polymers with a different periodicity and larger content of Gly as investigated in the present study. In fact, the CD difference spectrum of the poly-(Gly_4Ser) appendix investigated here has the typical appearance of a polypeptide in random coil conformation, whereby the chiral Ser residues served as a spectroscopic probe. Thus, we were possibly able to experimentally demonstrate for the first time a truly disordered structure for a glycine-rich polymer at ambient temperature in physiological solution.

As a consequence of the random chain character of the HAP fusion partner, the apparent hydrodynamic volume of the 4D5 Fab fragment could be more than doubled in the

case of the 200 residue version, as shown by gel permeation chromatography, although the polypeptide chain was only by 47% (i.e. 211 residues, including the C-terminal *Strep*-tag II) longer than that of the unfused Fab fragment (443 residues) and its molecular mass was just by 29% larger (i.e. 61 925 versus 48 004 g mol^{-1}). Hence, HAPylation is an efficient means to enhance the hydrodynamic volume of a small protein while retaining a high specific activity.

Using the theoretical principles of polymer biophysics, the random coil diameter of a chain of 200 Gly residues would amount to ca. 75 Å—calculated as the average root mean square end-to-end distance of $\sqrt{\langle r^2\rangle} = l\sqrt{(nC_\infty)}$, with $n =$ 200 rotatable bonds of length $l = 3.8$ Å for each C_α–C_α distance and the 'characteristic ratio' $C_\infty \approx 2.0$ for poly(Gly) (Brant *et al.*, 1967; Creighton, 1993). This is slightly larger than the average N to C distance of ~60 Å for the light and heavy chains of the 4D5 Fab fragment with an almost fully stretched elbow angle (PDB entry 1FVD) and corresponds nicely with the more than doubled hydrodynamic volume that was measured for the corresponding fusion protein via GPC. As a more commonly used parameter in biophysics, the radius of gyration $R_g = l\sqrt{(C_\infty n/6)}$ for the 200 residue HAP would amount to 31 Å.

These relations show that, in principle, there are two ways of extending the hydrodynamic volume of a random chain HAP: (i) by using a longer chain length as discussed above or (ii) by using amino acids that exhibit a larger characteristic ratio, C_∞. This parameter, which is a measure for the inherent stiffness of the molecular chain, has a value of 9 for most amino acids (Brant *et al.*, 1967), except for Gly, which lacks a side chain, and for the imino acid Pro. Consequently, Gly and Pro contribute to reducing the dimensions of random coil proteins (Miller and Goebel, 1968). Unfortunately, however, homo-polymers of most other amino acids adopt a soluble random chain at ambient temperature only in the presence of strong denaturants, such as urea or Gdn/HCl.

In this context, a comparison with PEG chains is of interest. Using published parameters for the polymer biophysics of PEG (Bhat and Timasheff, 1992) with the formula $R_g = l\sqrt{(\sigma/3)}$ and $l = 2.75$, where σ is the number of bonds (three per CH_2-CH_2-O- unit, having a molecular weight of 44 g mol^{-1}), a radius of gyration of 31 Å would correspond to a PEG chain with a molecular weight of 5600, which is in good agreement with static light scattering measurements (Devanand and Selser, 1991). This value is much smaller than the sizes of 20 000 or 40 000 (especially with branched versions of PEG), which are typically used to prolong the circulation of approved therapeutic proteins (Caliceti and Veronese, 2003; Harris and Chess, 2003).

Yet, when the pharmacokinetic effects of HAPylation on the 4D5 Fab fragment were studied *in vivo*, an extended plasma half-life was detected for the 200 residue HAP sequence. Notably, no detrimental effects were observed upon administration of the radioiodinated protein to mice, such as non-specific tissue uptake or deposition of aggregates. This shows that the fusion of a typical therapeutic protein with a random chain of 200 amino acids is tolerable to the organism and leads already to a significantly prolonged circulation time with a terminal half-life of ~6 h in mice. In fact, according to the principles of allometric scaling (Mahmood, 2005), even longer half-lives may be anticipated for humans. Furthermore, considerably larger effects should be expected when using HAP fusion proteins with at least double the hydrodynamic volume as was here achieved with the 200 residue Gly-rich HAP, finally aiming at surpassing the critical threshold of apparently 70 kDa for glomerular filtration.

Nevertheless, especially for radiolabeled probes which currently are widely investigated for *in vivo* molecular imaging purposes and radionuclide therapy (Gambhir, 2002; Kenanova and Wu, 2006), the differences in pharmacokinetic behavior already observed between the plain Fab fragment and its 200 residue HAP fusion could be of medical interest. Since the half-life of the radionuclides used for imaging studies are commonly in the range of 1–6 h, the delayed blood clearance observed for the HAPylated protein should result in a better bioavailability and thus higher target (e.g. tumor) uptake. Together with similar whole body levels at later time points (5–10 h), higher target/blood uptake ratios and thus better imaging contrast as well as higher therapeutic efficiency such as enhanced tumor activity would seem possible. It will be interesting to see in future studies if an adjustment between the clearance kinetics of HAPylated proteins in the early phase and the half-life of the radioisotope used for labeling can lead to advantages for *in vivo* imaging.

For purposes of comparison, we also applied a fusion protein between the 4D5 Fab fragment and a small bacterial ABD, which constitutes an alternative way of extending plasma half-life via complex formation with serum albumin. In this case, the terminal half-life was ca. 21 h, which is comparable to the value reported for fusion of the 4D5 Fab fragment with a short synthetic peptide ligand having albumin-binding activity (Nguyen *et al.*, 2006). This value is even longer than the 3–5 h elimination half-life so far reported for fusion proteins between the human soluble complement receptor type 1 and several ABDs of *Streptococcal* protein G in rats (Makrides *et al.*, 1996).

Interestingly, the amplitude of the distribution phase was much smaller in the case of the albumin association strategy mediated here by the ABD fusion partner and the AUC for blood clearance was much larger than for the other Fab fragments. In fact, this had to be expected as a consequence of the complex formation with serum albumin, whereby the recombinant fusion protein is largely retained in the plasma and only slowly released owing to the dynamic dissociation equilibrium. In contrast, the blood activity profile for the 200 residue HAP fusion indicates, similarly as for the conventional recombinant Fab fragment, that the large extravasal space is much better accessible in this case. Of course, more detailed pharmacokinetic studies will have to be carried out in order to quantify this effect. A better distribution of HAPylated proteins, compared with albumin fusion proteins or fusions with albumin-binding peptides, into the interstitial volume might turn out to provide advantages for therapeutic tissue targeting strategies.

It has to be emphasized that the experimental methodology chosen here, i.e. the *in vivo* comparison via radioiodination, should allow for a fairly exact determination of the clearance kinetics of the proteins. Yet, due to potential superposition of excretion and *in vivo* deiodination, the measured kinetic data might overvalue the real clearance rate. If the measured kinetics could be corrected for *in vivo* deiodination, the exact clearance rates are assumed to be somewhat slower, thus resulting in longer plasma half-lives. However, in the light of the good agreement of our pharmacokinetic data with several published

results, which were at least in part obtained with other methods of quantification (Nguyen *et al.*, 2006), this influence is probably low. Furthermore, based on our dual radioiodine-tracer technique, the comparison of trends and relations within the series of proteins investigated here ought to be fully valid.

In conclusion, we could show that it is possible to produce a recombinant protein, here an Fab fragment, which is even composed of two different polypeptide chains, as fusion with a long HAP of 200 residues that adopts a random coil conformation. The resulting protein is stable and fully functional in terms of antigen-binding activity. Its molecular sieving behavior in gel permeation chromatography suggests a considerably enhanced hydrodynamic volume, which is in agreement with the assumption of an attached random chain. Initial pharmacokinetic experiments resulted in a 3-fold slower elimination in mice. Hence, *in vivo* properties as they are typically conferred by PEGylation were, in principle, achieved by our HAPylation strategy. Future work with other HAP sequences and more extended polymer chains will show whether an even longer plasma half-life, ranging to several days, may be possible with this approach.

Acknowledgements

The authors wish to thank Uli Binder (TU München) for help in the characterization of some intermediate fusion protein constructs, Klaus Wachinger (TU München) for technical assistance during protein preparation, Walter Stelzer (TU München) for mass spectrometry and Tim Adams (CSIRO, Parkville, Australia) for providing the recombinant HER2/ErbB2 ectodomain.

References

Åkerström,B., Nielsen,E. and Björck,L. (1987) *J. Biol. Chem.*, **262**, 13388–13391.
Andrews,P. (1964) *Biochem. J.*, **91**, 222–233.
Bamford,C.H., Elliott,A. and Hanby,W.E. (1956) *Synthetic Polypeptides—Preparation, Structure, and Properties*, 2nd edn. Academic Press, New York.
Beck,E. and Zink,B. (1981) *Gene*, **16**, 35–58.
Bhat,R. and Timasheff,S.N. (1992) *Protein Sci.*, **1**, 1133–1143.
Bird,R.E. and Walker,B.W. (1991) *Trends Biotechnol.*, **9**, 132–137.
Brant,D.A., Miller,W.G. and Flory,P.J. (1967) *J. Mol. Biol.*, **23**, 47–65.
Breustedt,D.A., Schönfeld,D.L. and Skerra,A. (2006) *Biochim. Biophys. Acta*, **1764**, 161–173.
Bullock,W.O., Fernandez,J.M. and Short,J.M. (1987) *Biotechniques*, **5**, 376–378.
Caliceti,P. and Veronese,F.M. (2003) *Adv. Drug Deliv. Rev.*, **55**, 1261–1277.
Cantor,C.R. and Schimmel,P.R. (1980) *Biophysical Chemistry*, 2nd edn. W.H. Freeman and Company, New York.
Carter,P., *et al*. (1992a) *Bio/Technology*, **10**, 163–167.
Carter,P., Presta,L., Gorman,C.M., Ridgway,J.B., Henner,D., Wong,W.L., Rowland,A.M., Kotts,C., Carver,M.E. and Shepard,H.M. (1992b) *Proc. Natl Acad. Sci. USA*, **89**, 4285–4289.
Chapman,A.P. (2002) *Adv. Drug Deliv. Rev.*, **54**, 531–545.
Chen,D.Q. and Texada,D.E. (2006) *Gene Ther. Mol. Biol.*, **10A**, 1–12.
Cho,H.S., Mason,K., Ramyar,K.X., Stanley,A.M., Gabelli,S.B., Denney,D.W.,Jr. and Leahy,D.J. (2003) *Nature*, **421**, 756–760.
Clark,R., *et al*. (1996) *J. Biol. Chem.*, **271**, 21969–21977.
Colcher,D., Pavlinkova,G., Beresford,G., Booth,B.J., Choudhury,A. and Batra,S.K. (1998) *Q J Nucl Med*, **42**, 225–241.
Creighton,T.E. (1993) *Proteins–Structures and Molecular Properties*, 2nd edn. W. H. Freeman and Company, New York.
Del Tito,B.J., Jr., Ward,J.M., Hodgson,J., Gershater,C.J., Edwards,H., Wysocki,L.A., Watson,F.A., Sathe,G. and Kane,J.F. (1995) *J. Bacteriol.*, **177**, 7086–7091.
Dennis,M.S., Zhang,M., Meng,Y.G., Kadkhodayan,M., Kirchhofer,D., Combs,D. and Damico,L.A. (2002) *J. Biol. Chem.*, **277**, 35035–35043.
Devanand,K. and Selser,J.C. (1991) *Macromolecules*, **24**, 5943–5947.
Dieci,G., Bottarelli,L., Ballabeni,A. and Ottonello,S. (2000) *Protein Expr. Purif.*, **18**, 346–354.
Eigenbrot,C., Randal,M., Presta,L., Carter,P. and Kossiakoff,A.A. (1993) *J. Mol. Biol.*, **229**, 969–995.
Essen,L.-O. and Skerra,A. (1994) *J. Mol. Biol.*, **238**, 226–244.
Fändrich,M. and Dobson,C.M. (2002) *EMBO J.*, **21**, 5682–5690.
Ferl,G.Z., Kenanova,V., Wu,A.M. and DiStefano,J.J., III (2006) *Mol. Cancer Ther.*, **5**, 1550–1558.
Fiedler,M., Horn,C., Bandtlow,C., Schwab,M.E. and Skerra,A. (2002) *Protein Eng.*, **15**, 931–941.
Fling,S.P. and Gregerson,D.S. (1986) *Anal. Biochem.*, **155**, 83–88.
Gambhir,S.S. (2002) *Nat. Rev. Cancer*, **2**, 683–693.
Garrett,T.P., *et al*. (2003) *Mol. Cell*, **11**, 495–505.
Ghetie,V. and Ward,S. (2002) *Immunol. Res.*, **25**, 97–113.
Gill,S.C. and von Hippel,P.H. (1989) *Anal. Biochem.*, **182**, 319–326.
Goldenberg,M.M. (1999) *Clin. Ther.*, **21**, 75–87.
Greenfield,N. and Fasman,G.D. (1969) *Biochemistry*, **8**, 4108–4116.
Harris,J.M. and Chess,R.B. (2003) *Nat. Rev. Drug Discov.*, **2**, 214–221.
Hennecke,F., Krebber,C. and Plückthun,A. (1998) *Protein Eng.*, **11**, 405–410.
Holliger,P. and Hudson,P.J. (2005) *Nat. Biotechnol.*, **23**, 1126–1136.
Kenanova,V. and Wu,A.M. (2006) *Expert. Opin. Drug Deliv.*, **3**, 53–70.
König,T. and Skerra,A. (1998) *J. Immunol. Methods*, **218**, 73–83.
Kraulis,P.J., Jonasson,P., Nygren,P.Å., Uhlén,M., Jendeberg,L., Nilsson,B. and Kördel,J. (1996) *FEBS Lett.*, **378**, 190–194.
Mahmood,I. (2005) *Interspecies Pharmacokinetic Scaling. Principles and Application of Allometric Scaling*. Pine House Publishers, Rockville, MD.
Mahmood,I. (2006) *Clinical Pharmacology of Therapeutic Proteins*. Pine House Publishers, Rockville, MD.
Makrides,S.C., Nygren,P.Å., Andrews,B., Ford,P.J., Evans,K.S., Hayman,E.G., Adari,H., Uhlén,M. and Toth,C.A. (1996) *J. Pharmacol. Exp. Ther.*, **277**, 534–542.
Miller,W.G. and Goebel,C.V. (1968) *Biochemistry*, **7**, 3925–3935.
Nguyen,A., Reyes,A.E., II, Zhang,M., McDonald,P., Wong,W.L., Damico,L.A. and Dennis,M.S. (2006) *Protein Eng. Des. Sel.*, **19**, 291–297.
Novy,R., Drott,D., Yaeger,K. and Mierendorf,R. (2001) *Innovations*, **12**, 1–3.
Olsson,A., Eliasson,M., Guss,B., Nilsson,B., Hellman,U., Lindberg,M. and Uhlén,M. (1987) *Eur. J. Biochem.*, **168**, 319–324.
Osborn,B.L., Olsen,H.S., Nardelli,B., Murray,J.H., Zhou,J.X., Garcia,A., Moody,G., Zaritskaya,L.S. and Sung,C. (2002) *J. Pharmacol. Exp. Ther.*, **303**, 540–548.
Perry,C.M. and Wiseman,L.R. (1999) *Biodrugs*, **12**, 129–135.
Plückthun,A. and Skerra,A. (1989) *Methods Enzymol.*, **178**, 497–515.
Quadrifoglio,F. and Urry,D.W. (1968) *J. Am. Chem. Soc.*, **90**, 2760–2765.
Rippon,W.B. and Walton,A.G. (1971) *Biopolymers*, **10**, 1207–1212.
Rosendahl,M.S., Doherty,D.H., Smith,D.J., Bendele,A.M. and Cox,G.N. (2005) *Bioprocess Int.*, **3**, 52–61.
Sambrook,J., Fritsch,E.F. and Maniatis,T. (1989) *Molecular Cloning: A Laboratory Manual*. Cold Spring Harbor Laboratory Press, Cold Spring Harbor, New York.
Schiweck,W. and Skerra,A. (1995) *Proteins*, **23**, 561–565.
Schlapschy,M., Gruber,H., Gresch,O., Schäfer,C., Renner,C., Pfreundschuh,M. and Skerra,A. (2004) *Protein Eng. Des. Sel.*, **17**, 847–860.
Schulz,G.E. and Schirmer,R.H. (1979) *Principles of Protein Structure*. Springer, New York.
Shental-Bechor,D., Kirca,S., Ben-Tal,N. and Haliloglu,T. (2005) *Biophys. J.*, **88**, 2391–2402.
Skerra,A. (1994a) *Gene*, **151**, 131–135.
Skerra,A. (1994b) *Gene*, **141**, 79–84.
Skerra,A. and Schmidt,T.G. (2000) *Methods Enzymol.*, **326**, 271–304.
Skerra,A., Pfitzinger,I. and Plückthun,A. (1991) *Bio/Technology*, **9**, 273–278.
Squire,P.G. (1981) *J. Chromatogr. A*, **210**, 433–442.
Sreerama,N. and Woody,R.W. (2000) *Circular Dichroism—Principles and Applications*. Berova,N., Nakanishi,K. and Woody,R.W. (eds). John Wiley & Sons, New York, pp. 601–620.
Turner,D.J., Ritter,M.A. and George,A.J. (1997) *J. Immunol. Methods*, **205**, 43–54.
Viguera,E., Canceill,D. and Ehrlich,S.D. (2001) *J. Mol. Biol.*, **312**, 323–333.
Voss,S. and Skerra,A. (1997) *Protein Eng.*, **10**, 975–982.
Walsh,G. (2003) *Nat. Biotechnol.*, **21**, 865–870.
Yanisch-Perron,C., Vieira,J. and Messing,J. (1985) *Gene*, **33**, 103–119.

Received April 10, 2007; revised April 10, 2007; accepted April 17, 2007

Edited by Thomas Kiefhaber